Case Studies in Thermal Engineering 6 (2015) 40–51

Contents lists available at ScienceDirect

Case Studies in Thermal Engineering

journal homepage: www.elsevier.com/locate/csite

Investigation of heat transfer for cooling turbine disks with a non-Newtonian fluid flow using DRA

A.S. Dogonchi [a], D.D. Ganji [b,*]

[a] Mechanical Engineering Department, Mazandaran Institute of Technology, P.O. Box 747, Babol, Iran
[b] Mechanical Engineering Department, Babol Noshirvani University of Technology, P.O. Box 484, Babol, Iran

ARTICLE INFO

Article history:
Received 14 May 2015
Received in revised form
28 May 2015
Accepted 10 June 2015
Available online 12 June 2015

Keywords:
Non-Newtonian fluid flow
Porous media
Axisymmetric channel
Nusselt number
Duan–Rach Approach (DRA)
Adomian Decomposition Method (ADM)

ABSTRACT

A non-Newtonian viscoelastic fluid flow passes through the porous wall of an axisymmetric channel on a turbine disc for cooling application. The present article solves the couple equations (momentum and heat transfer) of a non-Newtonian fluid flow in an axisymmetric channel with a porous wall for turbine cooling applications by using the Duan–Rach Approach (DRA). The precious achievement of the present work is introducing a new and efficient approximate analytical technique that this method allows us to find a solution without using numerical methods to evaluate the undetermined coefficients. The approximate analytical investigation is carried out for different values of the embedding parameters namely: Reynolds number, Prandtl number, injection Reynolds number and power law index. The DRA results indicate that Nusselt number has direct relationship with Reynolds number, Prandtl number and power law index. Also the results were compared with numerical solution in order to verify the accuracy of the proposed method. It is seen that the current results in comparison with the numerical ones are in excellent agreement.

1. Introduction

The study of non-Newtonian fluid flow in the presence of porous media has become main interest in many engineering and industrial applications, particularly the interest in heat transfer problem of non-Newtonian fluids has grown considerably. Hot rolling, extrusion of plastics, flow in journal bearings, lubrication, flow in a shock absorber, ceramic processing, biomechanics, enhanced oil, recovery process, filtration process, polymer processing, electronic packing and drag reduction are some typical examples to name. Understanding the nature of channel flow of non-Newtonian fluid and related heat transfer problem by mathematical modeling with a view to predict the temperature distribution and the associated behavior of fluid flow have been the focus of considerable research works [1–7]. This problem can be modeled mathematically by nonlinear ordinary differential equation systems. The solution of this nonlinear problem is normally obtained by using, for example, the perturbation method [8]. In most cases, such problems will not admit analytical solution, and this necessitates the implementation of special techniques. In recent years, much attention has been devoted to the newly developed methods to construct an analytical solution of differential equation; such as Adomian Decomposition Method (ADM) [9,10], Differential Transformation Method (DTM) [11–15], etc.

* Corresponding author. Fax: +98 11 32334205
E-mail addresses: sattar.dogonchi@yahoo.com (A.S. Dogonchi), ddg_davood@yahoo.com (D.D. Ganji).

http://dx.doi.org/10.1016/j.csite.2015.06.002

Nomenclature

A, B	symmetric kinematic matrices
C	specific heat
C_n	blade – wall temperature coefficient
DRA	Duan–Rach approach
ADM	Adomian decomposition method
$\partial v_m/\partial x_n$	velocity gradients
$\partial a_m/\partial x_n$	acceleration gradients
x_k	general coordinate
f	velocity function
κ	fluid thermal conductivity
n	Power law index in temoerature distribution
Re	injection Reynolds number
K_r	rotation parameter
u_r, u_z	velocity components in r, z directions, respectively
NM	numerical
ρ	fluid density
T	temperature
$q_n(\eta)$	temperature function
Pr	Prandtl number
ψ	stream function
τ_{ij}	stress tensor component
P	fluid pressure
r, θ, z	cylindrical coordinate symbols
V	injection velocity
ϕ_k	viscosity coefficients
φ	dissipation function
η	dimensionless coordinate in z direction
ψ	stream function

Subsequently, several studies were performed on the heat transfer in the presence of porous media. The heat transfer and entropy generation in a channel partially filled with porous media using local thermal non-equilibrium model was studied by Torbabi et al. [16]. They discussed about the effects of many thermophysical parameters on the velocity, temperature, Nusselt number and entropy generation rates. The laminar fluid flow and heat transfer in channel with porous walls in the presence of a transverse magnetic field was investigated by Fakour et al. [17]. They applied the Least Square Method (LSM) to solve governing equations. Their results indicate that increasing the Reynolds and Hartman number is reduces the nanofluid flow velocity in the channel and the maximum amount of temperature increase and increasing the Prandtl and Eckert number will increase the maximum amount of temperature. Vahabzadeh et al. [18] studied the temperature distribution, heat transfer rate, efficiency and optimization of porous pin fins in fully wet conditions. They applied the Least Square Method (LSM) to solve governing equations. Their results indicate that the temperature distribution is increased by increasing the Relative Humidity (RH) percentage. The combined conduction–convection–radiation heat transfer in heat exchangers filled with a fluid saturated cellular porous medium was investigated by Dehghan et al. [19]. They applied the Homotopy Perturbation Method (HPM) to solve governing equations. Also, they discussed about the effects of porous medium shape parameter(s) and radiation parameters on the thermal performance. Pia and Sanna [20] studied the influence of microstructure voids on thermal conductivity in fractal porous media. They discussed about the effects of pore size, geometric organization and complexity of the porous media on the thermal conductivity. Their results indicate that the presence of pore walls and a great number of small pores decrease the value of thermal conductivity. Huai et al. [21] studied several types of fractals to model the structures of porous media, and heat conduction in these structures. They applied the finite volume method (FVM) to discretizing the governing equations. Also, they discussed about the effects of the porosity, the size and spatial distribution of pores on the effective thermal conductivity of these structures.

In 1986 Adomian [9] published an analytical method to solve nonlinear equations. Esmaili et al. [22] applied this technique to resolve the convergent–divergent flow. The results obtained show a good agreement with the numerical methods. Hashim [23] presented the Adomian Decomposition Method for solving boundary value problems for fourth-order integro-differential equations and the Blasius equation. Many authors have tried to modify the ADM. Jin [24] modified ADM for solving a kind of evolution equation. All these methods need to find the unknown initial values of the problem that the final solution depends on the accuracy of the initial values determined by numerical method. Duan et al. [25] have presented a new modification of the ADM that called Duan–Rach Approach (DRA), to solve a wide class of multi-order and multi-point nonlinear boundary value problems (BVP). Dib et al. [26] applied Duan–Rach Approach (DRA) to solve the magneto hydrodynamic (MHD) Jeffery–Hamel flow. The results obtained show a good agreement with the numerical method and homotopy analysis method (HAM). Also, Dib et al. [27] applied proposed method to obtain an approximate analytical solution of squeezing unsteady nanofluid flow between two parallel plates.

In the present work, we have applied this modified method (DRA) to solve equation of non-Newtonian fluid flow in an axisymmetric channel with a porous wall for turbine cooling applications and have made a comparison with the numerical solution in order to verify the accuracy of the proposed method. The numerical results of this problem have been performed using Maple14.

2. Flow and heat transfer analysis and mathematical formulation

This study is concerned with simultaneous development of flow and heat transfer for non-Newtonian viscoelastic fluid flow on the turbine disc for cooling purposes. The problem to be considered is depicted schematically in Fig. 1.The r-axis is

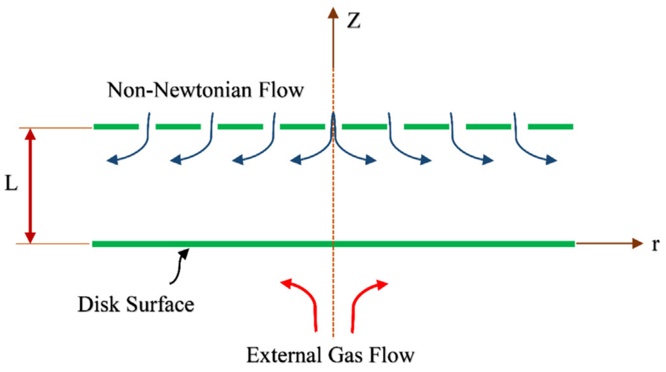

Fig. 1. Schematic view of the physical system.

parallel to the surface of disk and the z-axis is normal to it. The porous disc of the channel is at $z = +L$. The wall that coincides with the$r$-axis is heated externally and non-Newtonian fluid is injected uniformly from the other perforated wall in order to cool the heated wall. As can be observed in Fig. 1 the cooling problem of the disk can be considered as a stagnation point flow with injection. For a steady, axisymmetric, non-Newtonian fluid flow the following equations can be written in cylindrical coordinates. The continuity equation

$$\frac{\partial(ru_r)}{\partial r} + \frac{\partial(ru_z)}{\partial z} = 0 \tag{1}$$

and the momentum equations

$$u_r\frac{\partial u_r}{\partial r} + u_z\frac{\partial u_r}{\partial z} = -\frac{1}{\rho}\frac{\partial P}{\partial r} + \frac{1}{\rho}\left[\frac{\partial \tau_{rr}}{\partial r} + \frac{1}{r}(\tau_{rr} - \tau_{\theta\theta}) + \frac{\partial \tau_{rz}}{\partial z}\right] \tag{2}$$

$$u_r\frac{\partial u_z}{\partial r} + u_z\frac{\partial u_z}{\partial z} = -\frac{1}{\rho}\frac{\partial P}{\partial z} + \frac{1}{\rho}\left[\frac{\partial \tau_{rz}}{\partial r} + \frac{\tau_{rz}}{r} + \frac{\partial \tau_{zz}}{\partial z}\right] \tag{3}$$

and the energy equation

$$\rho C\left(u_r\frac{\partial T}{\partial r} + u_z\frac{\partial T}{\partial z}\right) = \kappa\nabla^2 T + \varphi \tag{4}$$

The analytical model under consideration leads to the following boundary conditions

$$z = 0:\ u_r = 0,\quad u_z = 0,\quad T = T_w \tag{5}$$

$$z = L:\ u_r = 0,\quad u_z = -V,\quad T = T_0 \tag{6}$$

In the above equations, u_r and u_z are the velocity components in the r and z directions, V is the injection velocity, ρ is the density, P is the pressure, T is the temperature, C is the specific heat, κ is the heat condition coefficient of the fluid, $\tau_{rr}, \tau_{rz}, \tau_{zr}, \tau_{zz}$ are the components of the stress matrix and φ is the dissipation function.

For particular class of viscoelastic and viscoinelastic fluids Rivlin [6] showed that if the stress components τ_{ij} at a point $x_k (k = 1, 2, 3)$ and at a time t are assumed to be polynomials in the velocity gradient $\frac{\delta v_m}{\delta x_n}(m, n = 1, 2, 3)$ and the acceleration gradients $\frac{\delta a_m}{\delta x_n}(m, n = 1, 2, 3)$ and in addition it is assumed to be isentropic the stress matrix can be expressed in the form

$$\|\tau_{ij}\| = \phi_0 I + \phi_1 A + \phi_2 B + \phi_3 A^2 + \ldots \tag{7}$$

Here I is the unit matrices, A and B are symmetric kinematic matrixes defined by

$$A = \left\|\frac{\delta v_i}{\delta x_j} + \frac{\delta v_j}{\delta x_i}\right\|,\qquad B = \left\|\frac{\delta a_i}{\delta x_j} + \frac{\delta a_j}{\delta x_i} + 2\frac{\delta v_m}{\delta x_i}\frac{\delta v_m}{\delta x_j}\right\| \tag{8}$$

and $\phi_k (k = 0, 1, 2, 3)$ are polynomials in the invariants of A, B, A^2. This study is restricted to second order fluids for which $\phi_k (k = 0, 1, 2, 3)$ are constant and $\phi_k (k = 4, 5, 6, \ldots)$ are zero. So that the stress components are as follows:

$$\tau_{rr} = \phi_1 A_{rr} + \phi_2 A_{rr}^2 + \phi_3 B_{rr} \tag{9}$$

$$\tau_{zz} = \phi_1 A_{zz} + \phi_2 A_{zz}^2 + \phi_3 B_{zz} \tag{10}$$

$$\tau_{\theta\theta} = \phi_1 A_{\theta\theta} + \phi_2 A_{\theta\theta}^2 + \phi_3 B_{\theta\theta} \tag{11}$$

$$\tau_{rz} = \phi_1 A_{rz} + \phi_2 A_{rz}^2 + \phi_3 B_{rz} \tag{12}$$

and the dissipation function is defined as

$$\varphi = \tau_{rr}\frac{\partial u_r}{\partial r} + \tau_{\theta\theta}\frac{u_r}{r} + \tau_{zz}\frac{\partial u_z}{\partial z} + \tau_{rz}\left(\frac{\partial u_r}{\partial z} + \frac{\partial u_z}{\partial r}\right) \tag{13}$$

For the solution of this problem in the case of axially symmetric flow it is convenient to define a stream function so that the continuity equation is satisfied

$$\psi = Vr^2 f(\eta) \tag{14}$$

where $\left(\eta = {}^{z}/_{L}\right)$ and the velocity components can be derived as

$$u_r = \frac{Vr}{L} f'(\eta) \tag{15}$$

$$u_z = -2Vf(\eta) \tag{16}$$

where prime denotes differentiation with respect to η. Using Eqs. (14)–(16) the equations of motion reduce to

$$f'^2 - 2ff'' = -\frac{L^2}{\rho V^2 r}\frac{\partial P}{\partial r} + \frac{\phi_1}{\rho VL} f''' + \frac{\phi_2}{\rho L^2}\left(f''^2 - 2f'f'''\right) + \frac{\phi_3}{\rho L^2}\left(f''^2 - 2ff^{iv}\right) \tag{17}$$

$$4ff' = -\frac{L^2}{\rho V^2}\frac{\partial P}{\partial z} - 2\frac{\phi_1}{\rho VL} f'' + 2\frac{\phi_2}{\rho L^2}\left(14f'f'' + \frac{r^2}{L} f''f'''\right) + 4\frac{\phi_3}{\rho L^2}\left(11f'f'' + ff''' + \frac{r^2}{L} f''f'''\right) \tag{18}$$

The pressure term can be eliminated by differentiating Eq. (17) with respect to z and Eq. (18) with respect to r and subtracting the resulting equations. This gives the following equations:

$$-2ff''' = \frac{f^{iv}}{Re} - K_1\left(4f''f''' + 2f'f^{iv}\right) - K_2\left(4f''f''' + 2f'f^{iv} + 2ff^{v}\right) \tag{19}$$

where $K_1 = {}^{\phi_2}/_{\rho L^2}$, $K_2 = {}^{\phi_3}/_{\rho L^2}$ is the injection Reynolds number. For $\phi_3 = 0$ the equation turned to

$$f^{iv} + 2Reff''' - K_1 Re\left(4f''f''' + 2f'f^{iv}\right) = 0 \tag{20}$$

The boundary conditions are

$$\eta = 0:\ f = 0,\ \ f' = 0 \tag{21}$$

$$\eta = 1:\ f = 1,\ \ f' = 0 \tag{22}$$

On the other hand, for equation of heat transfer, Letting the blade wall $(z = 0)$ temperature distribution be $T_w = T_0 + \sum_{n=0}^{\infty} C_n\left(\frac{r}{L}\right)^n$ and assuming the fluid temperature to have the form of [2]

$$T = T_0 + \sum_{n=0}^{\infty} C_n\left(\frac{r}{L}\right)^n q_n(\eta) \tag{23}$$

where T_0 is the temperature of the incoming coolant $(z = L)$ and neglecting dissipation effect the following non-dimensional equation and boundary conditions are obtained

$$nf'q_n - 2fq_n' = \frac{1}{PrRe} q_n'', \quad (n = 0, 2, 3, 4, \ldots) \tag{24}$$

$$\eta = 0:\ q_n = 1 \tag{25}$$

$$\eta = 1:\ q_n = 0 \tag{26}$$

3. Description of the Duan–Rach approach (DRA)

3.1. Fundamentals of the Adomian decomposition method (ADM)

Consider the following general functional equation:

$$u(x) - \mathrm{N}u(x) = f(x) \tag{27}$$

where N denotes a nonlinear operator and $f(x)$ is a known function. The ADM suggests the solution of Eq. (27) to be an infinite series form of

$$u(x) = \sum_{n=0}^{\infty} u_m(x) \tag{28}$$

and the nonlinear operator N to be decomposed as

$$\mathrm{N}u(x) = \sum_{n=0}^{\infty} A_m(x) \tag{29}$$

where

$$A_m(x) = A_n(u_0(x), u_1(x), \ldots, u_m(x)) \tag{30}$$

where the $A_m(x)$ are the Adomian polynomials, which can be determined by the formula

$$A_m(\eta) = \frac{1}{m!}\frac{d^m}{d\lambda^m}\left[N\left(\sum_{i=0}^{m} \lambda^i F_i(\eta)\right)\right]_{\lambda=0} \tag{31}$$

that was first published by Adomian and Rach [28].

3.2. Modified ADM by Duan–Rach approach

Consider a third-order non-linear differential equation

$$Lu = Nu + g(x), \tag{32}$$

subject to the mixed set of Dirichlet and Neumann boundary conditions

$$u(x_1) = \alpha_0,\ u'(x_1) = \alpha_1,\ u'(x_2) = \alpha_2,\ x_2 \neq x_1 \tag{33}$$

where $L = {}^{d^3}\!/_{dx^3}$ is the linear differential operator to be inverted, Nu is an analytic nonlinear operator, and $g(x)$ is the system input.

We take the inverse linear operator as

$$L^{-1}(\bullet) = \int_{x0}^{x}\int_{x1}^{x}\int_{\xi}^{x} (\bullet)dx\,dx\,dx, \tag{34}$$

where ξ is a prescribed value in the specified interval. Thus we have

$$L^{-1}Lu = u(x) - u(x_0) - u'(x_1)(x - x_0) - \frac{1}{2}u''(\xi)[(x - x_1)^2 - (x_0 - x_1)^2] \tag{35}$$

Applying the inverse operator L^{-1} to both sides of Eq. (32) yields

$$L^{-1}[Nu + g] = u(x) - u(x_0) - u'(x_1)(x - x_0) - \frac{1}{2}u''(\xi)[(x - x_1)^2 - (x_0 - x_1)^2] \tag{36}$$

We differentiate Eq. (35), then let $x = x_2$ and solve for $u''(\xi)$, hence

$$u``(\xi) = \frac{u`(x_2) - u`(x_1)}{x_2 - x_1} - \frac{1}{x_2 - x_1}\int_{x1}^{x2}\int_{\xi}^{x} [Nu + g]dx\,dx. \tag{37}$$

Substituting Eq. (37) into Eq. (36) yields,

$$u(x) = u(x_0) + u`(x_1)(x - x_0) + \frac{1}{2}\left[(x - x_1)^2 - (x_0 - x_1)^2\right]\frac{u`(x_2) - u`(x_1)}{x_2 - x_1} + L^{-1}g + L^{-1}Nu$$
$$- \frac{1}{2}\frac{(x - x_1)^2 - (x_0 - x_1)^2}{x_2 - x_1}\int_{x1}^{x2}\int_{\xi}^{x} g\,dx\,dx - \frac{1}{2}\frac{(x - x_1)^2 - (x_0 - x_1)^2}{x_2 - x_1}\int_{x1}^{x2}\int_{\xi}^{x} Nu\,dx\,dx. \tag{38}$$

Thus in Eq. (38) the three known boundary values $u(x_0)$, $u'(x_1)$ and $u'(x_2)$ are included and the undetermined coefficient was replaced. Next, the solution is decomposed and the nonlinearity $u(x)=\sum_{m=0}^{\infty}u_m(x)$, $Nu(x)=\sum_{m=0}^{\infty}A_m(x)$ where $A_m(x)=A_m(u_0(x),u_1(x),\ldots,u_m(x))$ are the Adomian polynomials.

From Eq. (37), the solution components are determined by the modified recursion scheme

$$u_0 = u(x_0) + u'(x_1)(x-x_0) + \frac{1}{2}\left[(x-x_1)^2-(x_0-x_1)^2\right]\frac{u'(x_2)-u'(x_1)}{x_2-x_1} + L^{-1}g - \frac{1}{2}\frac{(x-x_1)^2-(x_0-x_1)^2}{x_2-x_1}\int_{x_1}^{x_2}\int_{\xi}^{x} g\,dx\,dx, \tag{39}$$

$$u_{m+1} = L^{-1}A_m - \frac{1}{2}\frac{(x-x_1)^2-(x_0-x_1)^2}{x_2-x_1}\int_{x_1}^{x_2}\int_{\xi}^{x} A_m dx\,dx. \tag{40}$$

4. Implementation of the method

In our study, the Duan–Rach Approach must be modified. We do not use the prescribed value ξ.

According to Eq. (32), Eqs. (20) and (24) can be written as follows:

$$L_4 f = -2Reff''' + K_1Re\left(4f''f''' + 2f'f^{iv}\right) \tag{41}$$

$$L_2 q_n = PrRe\left(nf'q_n - 2fq_n'\right) \tag{42}$$

where the differential operator L_4 and L_2 are given by $L_4 = {d^4}/{d\eta^4}$ and $L_2 = {d^2}/{d\eta^2}$ respectively. Assume that the inverse operator L_4^{-1} and L_2^{-1} exist, then we have

$$L_4^{-1}(\bullet) = \int_0^{\eta}\int_0^{\eta}\int_0^{\eta}\int_0^{\eta}(\bullet)d\eta\,d\eta\,d\eta\,d\eta,\quad L_2^{-1}(\bullet) = \int_0^{\eta}\int_0^{\eta}(\bullet)d\eta\,d\eta \tag{43}$$

Operating with L_4^{-1} in Eq. (41) and after exerting boundary conditions on it

$$f(\eta) = f(0) + f'(0)\eta + f''(0)\frac{\eta^2}{2} + f'''(0)\frac{\eta^3}{6} + L_4^{-1}(N_1u). \tag{44}$$

Operating with L_2^{-1} in Eq. (42) and after exerting boundary conditions on it

$$q_n(\eta) = q_n(0) + q_n'(0)\eta + L_2^{-1}(N_2u). \tag{45}$$

where N_1u and N_2u are introduced as

$$N_1u = -2Reff''' + K_1Re\left(4f''f''' + 2f'f^{iv}\right), \tag{46}$$

$$N_2u = PrRe\left(nf'q_n - 2fq_n'\right). \tag{47}$$

Obviously, we do not have the values of $f''(0)$, $f'''(0)$ and $q_n'(0)$. In the standard Adomian decomposition method (ADM), we need to evaluate those unknown conditions with numerical methods. Consequently, the boundary value problem (BVP) is turned into an initial value problem (IVP). The accuracy of the solution depends on the accuracy of the three unknown parameters. In our study, we use the Duan–Rach Approach [25] to find a totally analytical solution.

Operating with L_4^{-1} on Eq. (41) at $\eta=1$, we have

$$\int_0^1\int_0^{\eta}\int_0^{\eta}\int_0^{\eta} f^{iv}(\eta)d\eta\,d\eta\,d\eta\,d\eta = \left[L_4^{-1}N_1u\right]_{\eta=1}, \tag{48}$$

where

$$\left[L_4^{-1}N_1u\right]_{\eta=1} = \int_0^1\int_0^{\eta}\int_0^{\eta}\int_0^{\eta}(N_1u)d\eta\,d\eta\,d\eta\,d\eta \tag{49}$$

After integration of the left hand side, we have

$$1 - \frac{1}{2}f''(0) - \frac{1}{6}f'''(0) = \left[L_4^{-1}N_1u\right]_{\eta=1}. \tag{50}$$

Operating with L_3^{-1} on Eq. (41) at $\eta=1$, we have

Table 1
Comparison between DRA and numerical results.

η	f (when $Re=1$, $K_1=0.01$)			q_n (when $Re=1$, $K_1=0.02$, $Pr=1$, $n=0$)		
	DRA	NM	% Error	DRA	NM	% Error
0	0	0	0	1	1	0
0.1	0.031188982	0.03118898	7.35251E−06	0.869030364	0.869030359	5.53147E−09
0.2	0.114810882	0.114810875	6.40733E−06	0.738985402	0.738985392	1.34769E−08
0.3	0.235836971	0.235836956	6.12873E−06	0.611963412	0.611963396	2.53413E−08
0.4	0.379379585	0.379379563	5.59066E−06	0.490827836	0.490827813	4.74529E−08
0.5	0.531129975	0.53112995	4.61866E−06	0.378547137	0.378547101	9.43771E−08
0.6	0.677805204	0.677805183	3.08103E−06	0.277562244	0.277562198	1.68247E−07
0.7	0.807510276	0.807510267	1.14864E−06	0.189343984	0.189343939	2.39818E−07
0.8	0.909951115	0.909951117	2.35202E−07	0.114237788	0.114237769	1.71124E−07
0.9	0.976480301	0.976480301	2.05707E−08	0.051582243	0.05158225	1.23226E−07
1	1	1	0	0	0	0

$$\int_0^1 \int_0^\eta \int_0^\eta f^{iv}(\eta)d\eta\, d\eta\, d\eta = \left[L_3^{-1}N_1u\right]_{\eta=1}, \tag{51}$$

where

$$\left[L_3^{-1}N_1u\right]_{\eta=1} = \int_0^1 \int_0^\eta \int_0^\eta (N_1u)d\eta\, d\eta\, d\eta \tag{52}$$

After integration of the left hand side, we have

$$-f''(0) - \frac{1}{2}f'''(0) = \left[L_3^{-1}N_1u\right]_{\eta=1}. \tag{53}$$

The subtraction of Eq. (50) from Eq. (53) gives us the relation of $h'''(0)$

$$f'''(0) = 12\left[L_4^{-1}N_1u\right]_{\eta=1} - 12 - 6\left[L_3^{-1}N_1u\right]_{\eta=1} \tag{54}$$

and $h''(0)$ is

$$f''(0) = -\,6\left[L_4^{-1}N_1u\right]_{\eta=1} + 6 + 2\left[L_3^{-1}N_1u\right]_{\eta=1} \tag{55}$$

Substituting $f''(0)$ and $f'''(0)$ into Eq. (44) yields,

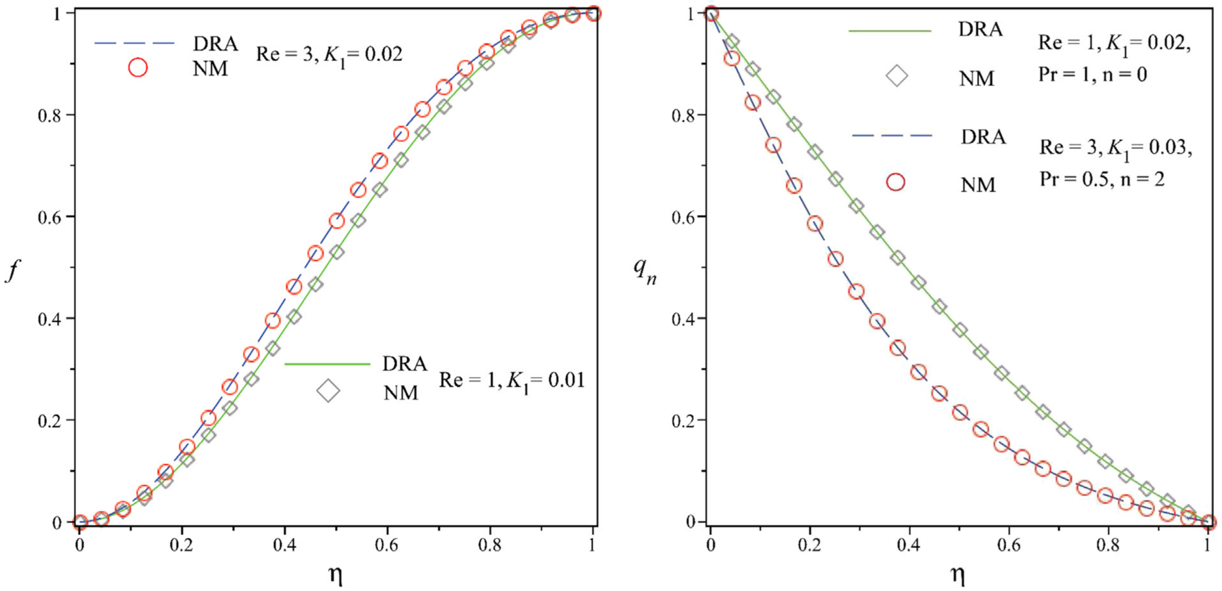

Fig. 2. Comparison of f and q_n obtained by DRA with numerical solution (NM).

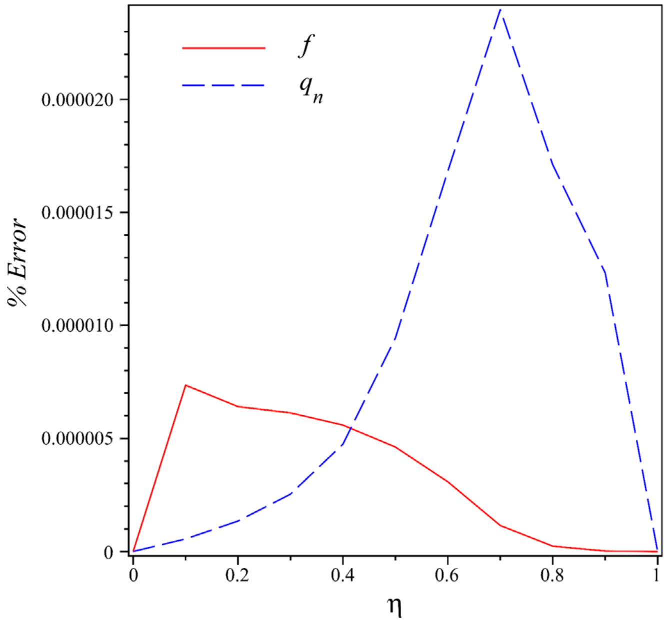

Fig. 3. Error (%) of DRA in comparison by the numerical solution for f (when $Re=1$, $K_1=0.01$) and q_n (when $Re=1$, $K_1=0.02$, $Pr=1$, $n=0$).

$$f(\eta)=3\eta^2-2\eta^3+\left(2\eta^3-3\eta^2\right)\left[L_4^{-1}N_1u\right]_{\eta=1}+\left(\eta^2-\eta^3\right)\left[L_3^{-1}N_1u\right]_{\eta=1}+\left[L_4^{-1}N_1u\right] \tag{56}$$

Thus the right hand side of Eq. (56) does not contain the undetermined parameters $f''(0)$ and $f'''(0)$.
Finally, we have the modified recursive scheme

$$f_0(\eta)=3\eta^2-2\eta^3$$

$$f_{m+1}(\eta)=\left(2\eta^3-3\eta^2\right)\left[L_4^{-1}A_m(\eta)\right]_{\eta=1}+\left(\eta^2-\eta^3\right)\left[L_3^{-1}A_m(\eta)\right]_{\eta=1}+\left[L_4^{-1}A_m(\eta)\right] \tag{57}$$

where the $A_m(\eta)$ are the Adomian polynomials, which can be determined by the formula.
Applying Eq. (31), we obtain the terms of the Adomian polynomials and put them in Eq. (57), and we determine $f_m(\eta)$ as follows:

$$f_0(\eta)=3\eta^2-2\eta^3$$

$$f_1(\eta)=\left(\frac{13}{35}Re-\frac{12}{5}K_1Re\right)\eta^2+\left(\frac{48}{5}K_1Re-\frac{18}{35}Re\right)\eta^3$$
$$-12K_1Re\cdot\eta^4+\frac{24}{5}K_1Re\cdot\eta^5+\frac{1}{5}Re\cdot\eta^6-\frac{2}{35}Re\cdot\eta^7 \tag{58}$$

The functions $f_2(\eta)$, $f_3(\eta)$, ⋯ can be determined in a similar way from Eq. (57). For convenience, we do not represent all terms of $f_n(\eta)$.
Using
$f(\eta)=\sum_{m=0}^{\infty}f_m(\eta)=f_0(\eta)+f_1(\eta)+f_2(\eta)+\ldots$Thus

$$f(\eta)=3\eta^2-2\eta^3+\left(\frac{13}{35}Re-\frac{12}{5}K_1Re\right)\eta^2+\left(\frac{48}{5}K_1Re-\frac{18}{35}Re\right)\eta^3$$
$$-12K_1Re\cdot\eta^4+\frac{24}{5}K_1Re\cdot\eta^5+\frac{1}{5}Re\cdot\eta^6-\frac{2}{35}Re\cdot\eta^7+-\ldots \tag{59}$$

According to Eq. (59), the accuracy increases by increasing the number of solution terms (n). For $q_n(\eta)$, we proceed in the same manner. We get the following recursive scheme:

$$q_{n,0}(\eta)=1-\eta$$

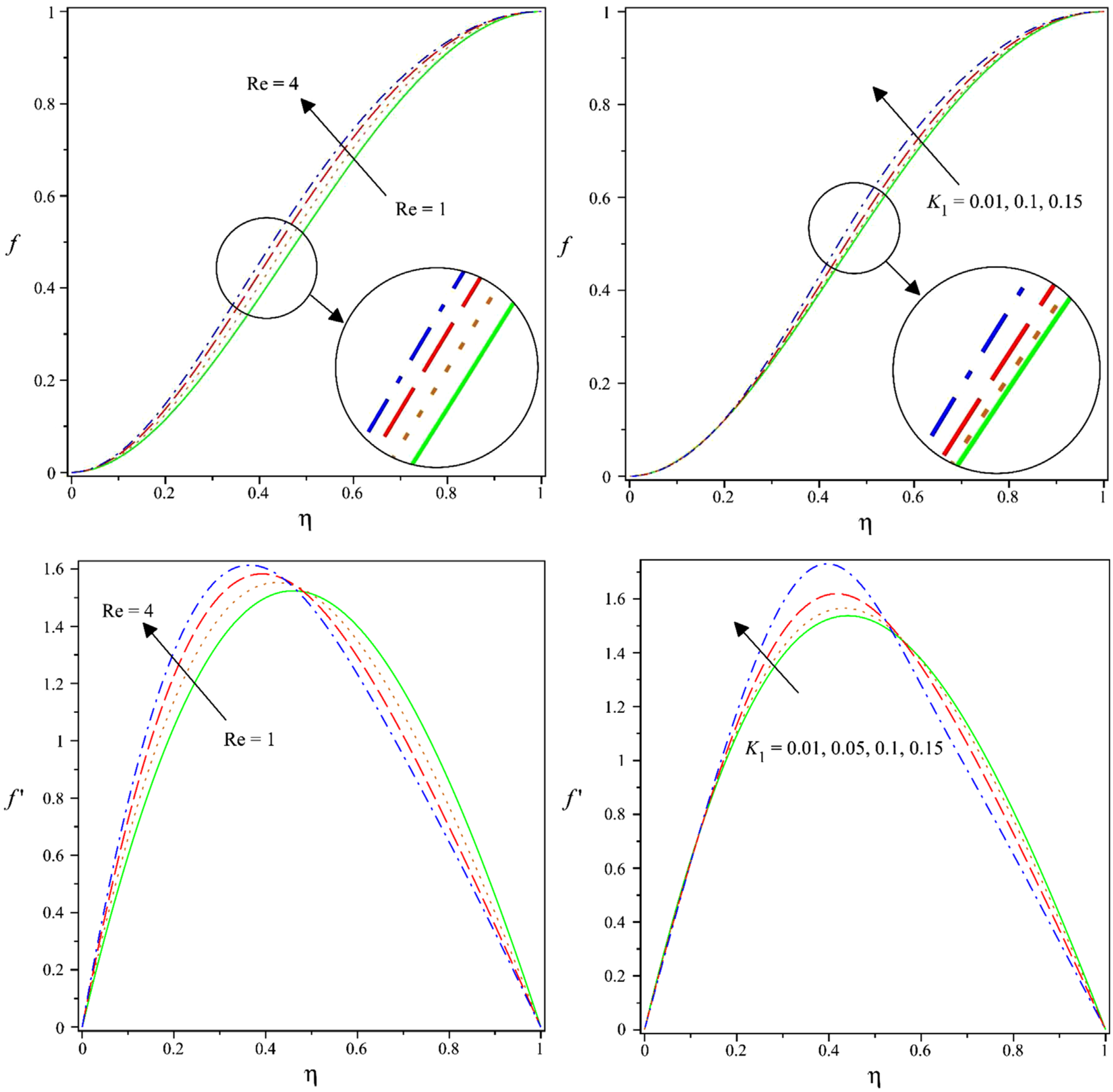

Fig. 4. Velocity profiles f and f' for different values of Re, K_1.

$$q_{n,m+1}(\eta) = -\eta\left[L_2^{-1}N_2 u\right]_{\eta=1} + \left[L_2^{-1}N_2 u\right] \tag{60}$$

where $\left[L_2^{-1}N_2 u\right]_{\eta=1} = \int_0^1 \int_0^\eta (N_2 u) d\eta\, d\eta$
using
$q_n(\eta) = \sum_{m=0}^{\infty} q_{n,m}(\eta) = q_{n,0}(\eta) + q_{n,1}(\eta) + q_{n,2}(\eta) + \ldots$thus

$$q_n(\eta) = 1 - \eta - \left(\frac{3}{10}Pr\cdot Re\cdot n + \frac{3}{10}Pr\cdot Re\right)\eta + Pr\cdot Re\cdot n\cdot\eta^3 + \left(\frac{1}{2}Pr\cdot Re - Pr\cdot Re\cdot n\right)\eta^4 + \left(\frac{3}{10}Pr\cdot Re\cdot n - \frac{1}{5}Pr\cdot Re\right)\eta^5 + - \ldots \tag{61}$$

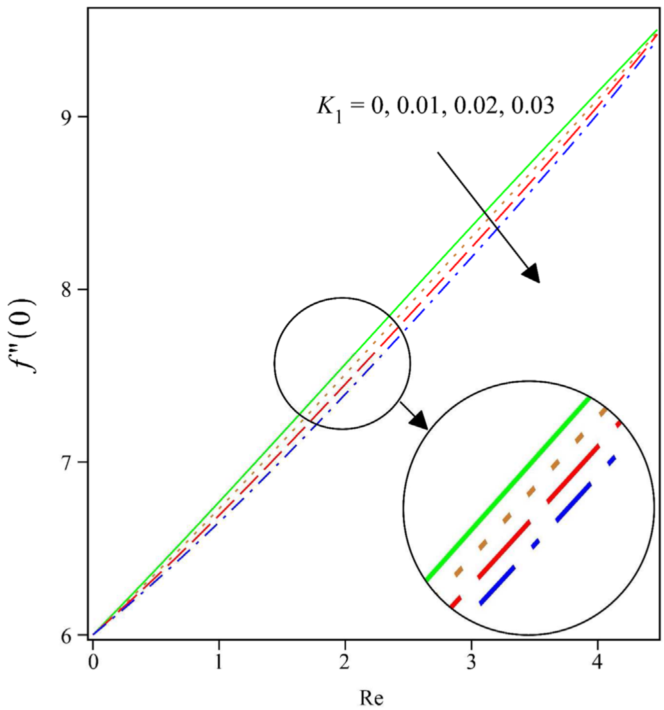

Fig. 5. Skin friction profile ($f''(0)$) under the effect of Re, K_1.

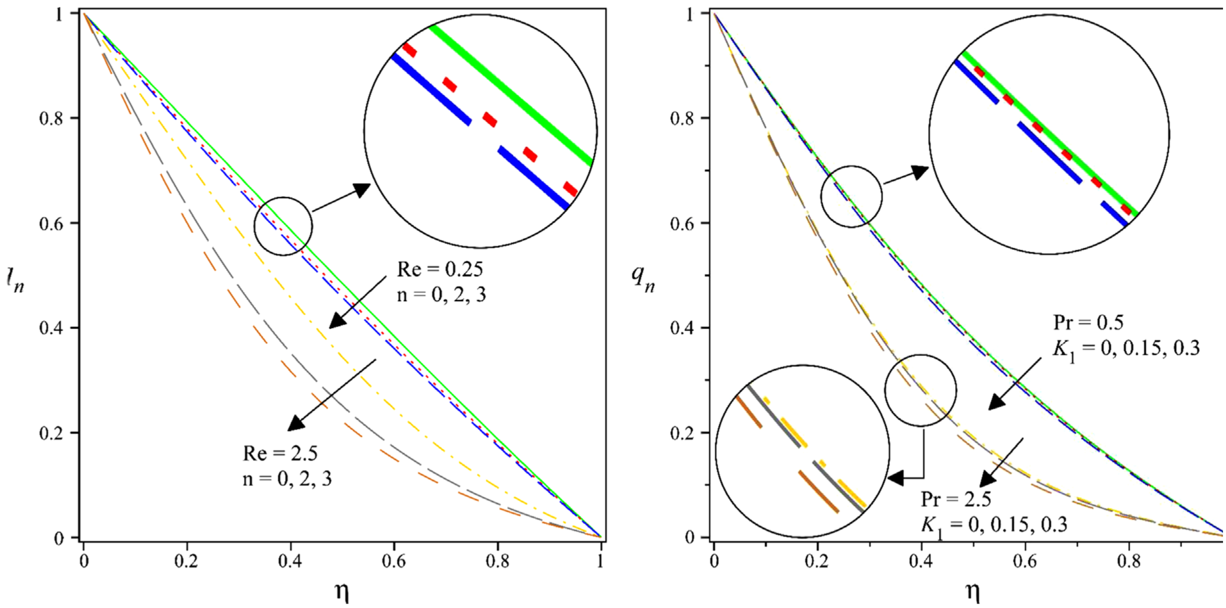

Fig. 6. Temperature distribution (q_n) for different values of Re, Pr, K_1, n.

5. Results and discussion

In this study, the heat transfer investigation of a non-Newtonian fluid flow in an axisymmetric channel with a porous wall for turbine cooling applications is considered using DRA (Fig. 1). The effects of various parameters such as the cross viscosity parameter (K_1), the power law index (n), the injection Reynolds number (Re) and the Prandtl number (Pr) are investigated on the velocity and temperature distribution. To validate the analytical results, we compare the analytical results with those of obtained by numerical solution for different values of the embedding parameters. The results are well

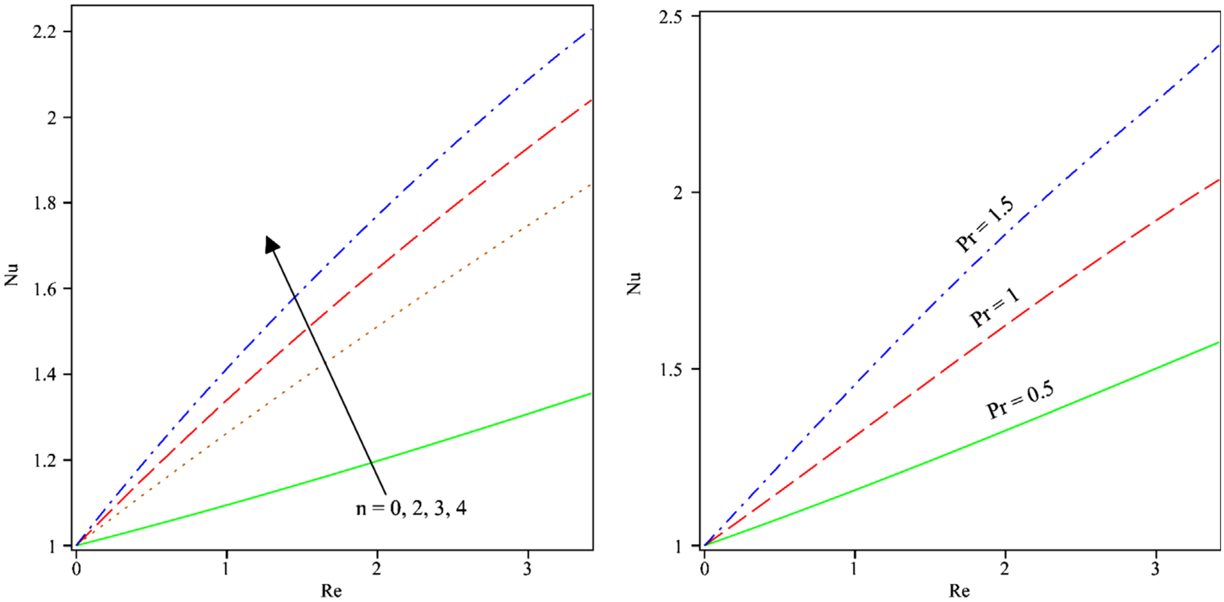

Fig. 7. dimensionless heat transfer rate (Nusselt number) for different values of *Re*, *Pr*, *n*.

matched with the results carried out by numerical solution as shown in Table 1 and Fig. 2. In Table 1, an error is introduced as follows:

$$\%\,Error = \left|\frac{DRA - NM}{NM}\right| \times 100.$$

Fig. 3 shows the Error (%) of the DRA in comparison to the numerical method and a low maximum Error (%) in this figure emphasis on accuracy and efficiency of the Duan–Rach Approach (DRA). This accuracy gives high confidence in the validity of this problem, and reveals an excellent agreement in engineering accuracy.

The effects of injection Reynolds number (*Re*) and K_1 on velocity profiles are shown in Fig.4. According to this figure, at low injection Reynolds numbers the velocity distribution exhibit center line symmetry indicating a Poiseuille flow for non-Newtonian fluids. At higher injection Reynolds numbers the location of the maximum velocity point tend to move closer to the solid wall where shear stress becomes larger as the injection Reynolds number grows. Also, as the K_1 increases, these effects become more conspicuous.

Fig. 5 shows the variation of the skin friction ($f'''(0)$) with *Re* number for constant values of K_1. One can observe that for constant values of K_1, $f'''(0)$ varies linearly with *Re* number and for constant value of the *Re* number, skin friction decreases with increasing value of K_1. Since $f'''(0)$ is measure of friction force, it is advisable to use viscoinelastic fluids as a coolant fluid for industrial gas turbine engines.

In Fig. 6 temperature distribution for different values of Reynolds number, Prandtl number, cross viscosity parameter (K_1) and power law index (n) are shown. One can observe that as Reynolds number, Prandtl number, cross viscosity parameter and power law index (n) increase, the $q_n(\eta)$ decreases. Also, as Reynolds number and power law index increase, the thermal boundary layer thickness decreases. This reduction causes to increase the Nusselt number. On the other hand, as seen in Fig. 6, the $q_n(\eta)$ variation is more gradual than when the power law index at a lower value or cross viscosity parameter at a higher value.

Fig. 7 shows the effect of the *Re* number, Prandtl number and power law index on the dimensionless heat transfer rate (Nusselt number, $Nu = -q'_n(0)$). As previously mentioned, As Reynolds number, Prandtl number and power law index increases the thermal boundary layer thickness decreases. Whereas Nusselt number has a inverse relation with boundary layer thickness, so with an increase in the *Re* number, Prandtl number and power law index the Nusselt number increases and that is final goal of this process to have a better cooling in the industrial application. Also, as seen in Fig. 7, the dimensionless heat transfer rate (Nusselt number) variation is more gradual than when the power law index at a lower value.

As previously mentioned, Figs. 2 and 3 confirm that the approach used is of a high accuracy for different Reynolds number (*Re*), Prandtl number (*Pr*), cross viscosity parameter (K_1) and power law index (n). In the ADM, for given *Re*, *Pr*, K_1 and n we have to solve $f(1)=1$, $f''(1)=0$ and $q_n(1)=0$ to find $\alpha_1=f'''(0)$, $\alpha_2=f'''(0)$ and $\beta=q'_n(0)$. If we change the value of *Re*, we have to again evaluate the values of α_1, α_2 and β. In our work (Duan–Rach Approach), the obtained solutions for $f(\eta)$ (Eq. (59)) and $q_n(\eta)$ (Eq. (61)) are purely analytic approach and we do not need any other calculations if we change any of parameters of the flow and the final solution does not contain undetermined coefficients.

6. Conclusions

In this paper, the Duan–Rach Approach (DRA) was used to obtain a purely approximate analytical solution of non-Newtonian fluid flow in an axisymmetric channel with a porous wall for turbine cooling applications. The Duan–Rach Approach allows us to find an analytical solution without using a numerical methods to evaluate the missing parameters $f''(0)$, $f'''(0)$ and $q'_n(0)$. The comparison between DRA and NM confirms the validity of this approach. The results show that the Nusselt number has direct relationship with Reynolds number, Prandtl number and power law index.

References

[1] White JL, Metzner AB. Constitutive equations for viscoelastic fluids with application to rapid external flows. AIChE J. 1965;11(2):324–30.
[2] Debruge LL, Han LS. Heat transfer in a channel with a porous wall for turbine cooling application. J. Heat Transf. Trans. ASME 1972;11:385–90.
[3] Shin S, Ahn HH, Cho YI, Sohn CH. Heat transfer behavior of a temperature dependent non-Newtonian fluid with Reiner–Rivlin model in a 2:1 rectangular duct. Int. J. Heat Mass Transf. 1999;42:2935–42.
[4] Böhme G. Non-Newtonian Fluid Mechanics. North Holland: Amsterdam; 1981.
[5] Akay M, Yükselen MA. Drag reduction of a non-Newtonian fluid by fluid injection on a moving wall. Arch. Appl. Mech. 1999;69(3):215–25.
[6] Rivlin RS, Ericksen JL. Stress–deformation relations for isotropic materials. J. Ration. Mech. Anal. 1955;4:323–425.
[7] Yuan SW, Finkelstein AB. Laminar pipe flow with injection and suction through a porous wall. Trans. ASME 1956;78:719–24.
[8] Kurtcebe C, Erim MZ. Heat transfer of a non-Newtonian viscoinelastic fluid in an axisymmetric channel with a porous wall for turbine cooling application. Int. Commun. Heat Mass Transf. 2002;29(7):971–82.
[9] Adomia G. Nonlinear Stochastic Operator Equations. New York: Academic Press; 1986.
[10] Sheikholeslami M, Ganji DD, Ashorynejad HR, Rokni HB. Analytical investigation of Jeffery-Hamel flow with high magnetic field and nanoparticle by Adomian decomposition method. Appl. Math. Mech. (Engl. Ed.) 2012;33(1):25–36.
[11] Zhou JK. Differential Transformation Method and its Application for Electrical Circuits. Wuhan, China: Hauzhang University Press; 1986.
[12] Dogonchi AS, Hatami M, Domairry G. Motion analysis of a spherical solid particle in plane Couette Newtonian fluid flow. Powder Technol. 2015;274: 186–92.
[13] Ganji DD, Dogonchi AS. Analytical investigation of convective heat transfer of a longitudinal fin with temperature-dependent thermal conductivity, heat transfer coefficient and heat generation. Int. J. Phys. Sci. 2014;9(21):466–74.
[14] Dogonchi AS, Hatami M, Hosseinzadeh Kh, Domairry G. Non-spherical particles sedimentation in an incompressible Newtonian medium by Padé approximation. Powder Technol. 2015;278:248–56.
[15] Hatami M, Ganji DD. Motion of a spherical particle in a fluid forced vortex by DQM and DTM. Particuology 2014;16:206–12.
[16] Torabi Mohsen, Zhang Kaili, Yang Guangcheng, Wang Jun, Wu Peng. Heat transfer and entropy generation analyses in a channel partially filled with porous media using local thermal non-equilibrium model. Energy 2015;82:922–38.
[17] Fakour M, Ganji DD, Abbasi M. Scrutiny of underdeveloped nanofluid MHD flow and heat conduction in a channel with porous walls. Case Stud. Therm. Eng. 2014;4:202–14.
[18] Vahabzadeh A, Ganji DD, Abbasi M. Analytical investigation of porous pin fins with variable section in fully-wet conditions. Case Stud. Therm. Eng. 2015;5:1–12.
[19] Dehghan Maziar, Rahmani Yousef, Domiri Ganji Davood, Saedodin Seyfollah, Sadegh Valipour Mohammad, Rashidi Saman. Convection–radiation heat transfer in solar heat exchangers filled with a porous medium: Homotopy perturbation method versus numerical analysis. Renew. Energy 2015;74: 448–55.
[20] Pia Giorgio, Sanna Ulrico. Case studies on the influence of microstructure voids on thermal conductivity in fractal porous media. Case Stud. Therm. Eng. 2014;2:8–13.
[21] Huai Xiulan, Wang Weiwei, Li Zhigang. Analysis of the effective thermal conductivity of fractal porous media. Appl. Therm. Eng. 2007;27:2815–21.
[22] Esmaili Q, Ramiar A, Alizadeh E, Ganji DD. An approximation of the analytical solution of the Jeffery-Hamel flow by decomposition method. Phys. Lett. A 2008;372:3434–9.
[23] Hashim I. Adomian decomposition method for solving BVPs for fourth-order integro-differential equations. J. Comput. Appl. Math. 2006;193:658–64.
[24] Jin C, Liu M. A new modification of adomian decomposition method for solving a kind of evolution equation. Appl. Math. Comput. 2005;169:953–62.
[25] Duan JS, Rach R. A new modification of the adomian decomposition method for solving boundary value problems for higher order nonlinear differential equations. Appl. Math. Comput. 2011;218:4090–118.
[26] Dib A, Haiahem A, Bou-said B. An analytical solution of the MHD Jeffery–Hamel flow by the modified Adomian decomposition method. Comput. Fluids 2014;102:111–5.
[27] Dib A, Haiahem A, Bou-said B. Approximate analytical solution of squeezing unsteady nanofluid flow. Powder Technol. 2015;269:193–9.
[28] Adomian G, Rach R. Inversion of nonlinear stochastic operators. J. Math. Anal. Appl. 1983;91:39–46.